Carlos M. PISCAL A.[1] and Francisco LÓPEZ-ALMANSA[2]

ABSTRACT (150 to 250 words)

The damping modification factors are utilized to alter the design spectral ordinates for constructions whose damping differs significantly from 5%, this being the level that is routinely considered by most codes. Such factors are habitually evaluated after suites of historical inputs representing the local seismicity. However, such records may not be readily available, due either to moderate seismicity or to limited seismological network; in such cases, representative artificial accelerograms might be used instead. This paper proposes a methodology for establishing damping modification factors after artificial inputs generated to match the 5% design spectra; this approach can be used for countries, regions or cities. The proposed methodology is based on performing dynamic analyses on underdamped and overdamped SDOF linear systems by using the aforementioned selected accelerograms. Although previous studies have highlighted the differences among factors generated after natural and artificial inputs, it has been observed that such discrepancies are mainly due to the longest significant (Trifunac) duration of the artificial accelerograms. Therefore, the artificial inputs are generated as their duration fits those of the available local strong motion records. An application to Colombia is presented; the results are compared with those for some available Colombian records. The sensitivity of the calculated factors to the soil type, period and seismic zone is investigated; matching expressions are provided. Such expressions are compared with the prescriptions of major design codes and with other studies. The suitability of the proposed formulation is further verified in an example on an isolated hospital building.

Keywords: Damping modification factor; artificial inputs; seismic isolation; code design spectrum; seismicity; Colombia

1 INTRODUCTION

A considerable number of seismic regulations merely provide design spectra corresponding to 5% damping. This damping level can be adequate for most of highly-damaged ordinary buildings and for some bridges, but the behavior of numerous other constructions is better described with significantly different damping ratios. Relevant examples of lower damping are: modern high-tech high-rise steel buildings, towers, masts, chimneys, racking systems, most of bridges (mainly the steel ones), steel warehouses, steel tanks, silos, arch and gravity dams, nuclear power plants, industrial facilities and buildings, pipelines, underground structures in rock or stiff soil, higher vibration modes of buildings with base isolation, and virtually all the undamaged constructions (i.e. assessment of damage limitation state in performance-based seismic engineering), among other cases. Regarding higher damping, there is also a considerable number of situations: old masonry buildings, timber constructions, most historic buildings, short bridges founded on soft soil, embankments, earth dams, underground structures in soft soil, buildings or bridges with base isolation, and buildings equipped with additional dampers, among other cases. Also, the substitute structure concept [Gulkan, Sozen 1974; Shibata, Sozen 1976], the Direct Displacement-based Design approach [Priestley 2003] and the Capacity Spectrum Method [ATC-40 1996], require the consideration of high damping over long period ranges. In this wide range of cases, considerable variations of the damping ratio are observed, ranging approximately between 0.5% and 30%, or higher. Using 5% damping spectra for constructions with different damping ratios can lead to important errors. If the damping ratio is less than 5%, the error lies on the unsafe side. In the opposite situation, the error is on the safe side; nonetheless, in base isolated constructions and in buildings with energy dissipators, the higher damping cannot be ignored,

[1] Civil Engineering Department, La Salle University, Bogotá, Colombia, cpiscal@unisalle.edu.co
[2] Professor, Technical University of Catalonia, Barcelona, francesc.lopez-almansa@upc.edu

given that is an essential part of the design. To sum up, it is strongly necessary to have seismic design spectra corresponding to a wide range of damping ratios.

Numerous seismic regulations provide criteria to modify the 5% damping spectral ordinates in order to match other damping levels; such criteria are commonly expressed in terms of damping modification factors intended to multiply the spectral ordinates. Some codes [EN-1998 2004; BSL 2009; GB 50011 2010; NCH 2745 2013] propose expressions or tables for modification factors to be considered for any other damping ratios. Conversely, the American regulations [ASCE 7-10 2010; FEMA P-1050 2016] provide modification factors that are intended only for buildings with base isolation or additional dampers; therefore, such coefficients can be solely employed for damping ratios higher than 5%. These correction coefficients have been derived [Ramírez et al. 2001; Ramírez et al. 2002] after seismic inputs recorded in the USA; the study [Sáez et al. 2012] for Chile [NCh2745 2013] has shown significant discrepancies with the American regulations [Piscal, López Almansa 2016; Piscal A. 2018]. Although these discrepancies can be partly explained by the varying assumptions, they rely mainly on the particularities of the seismicity of each country. These considerations show that the criteria for modifying the 5% design spectrum derived for a specific country cannot be extrapolated to other areas. Consequently, both this paragraph and the previous one highlight that there is a strong need for developing damping modification factors in countries where they are not currently available.

The damping modification factors are normally derived after strong historical seismic records that characterize the local seismicity. However, in numerous occasions this approach is unfeasible, given that the number of such records that are readily available is insufficient; this usually occurs when the seismicity is moderate (or medium) and the seismological network is limited. For such cases, two types of approaches have been proposed: using representative artificial accelerograms to compensate the scarcity of actual inputs, and retrieving real accelerograms from a database and modifying them to match the target spectrum. The second approach seems adequate for particular studies (i.e. for a given structure); conversely, in any general study, the spectral ordinates should be modified for the whole range of periods, this being rather unfeasible. In the framework of the first approach, this paper proposes a methodology for establishing damping modification factors (for countries, regions or cities) after artificial seismic inputs.

The proposed methodology starts by generating artificial accelerograms that are the fitted to the 5% damped code design spectra. Then, dynamic analyses on SDOF linear systems using such inputs are carried out. Finally, for a given damping ratio, the damping modification factor is defined as the ratio between the individual displacement spectral ordinates corresponding to such damping ratio and to 5%. For the sake of further reliability, the obtained factors are compared with those derived after the available local historical accelerograms. Perhaps the main objection to this approach is that previous researches [Bommer et al. 2005; Stafford et al. 2008; Hatzigeorgiou 2010] have underlined the differences among factors generated after natural and artificial inputs. However, such discrepancies are mainly due to the usual longest significant (Trifunac [Trifunac, Brady 1975]) duration of the artificial accelerograms. Therefore, in the proposed methodology, the artificial inputs are generated caring that their duration approximates those of the available local records. In any case, even if the consideration of artificial inputs may introduce some errors, they will be significantly smaller than using damping modification factors derived for foreign seismic conditions.

An example of application of the proposed strategy to Colombia is presented. In such application, the country is divided into ten seismic zones according to the current design code [NSR-10 2010], and the five most common soil types (A, B, C, D and E) are considered. Given the rather moderate seismicity of Colombia and the limitations and recentness of the seismological network, the available natural severe inputs are scarce. On the other hand, there is not enough information for selecting international records representing the Colombian hazard, such as moment magnitude and hypocentral distance. As well, as discussed in the previous paragraph, it is not possible to find records that can be scaled to the design spectra for the full range of periods. Therefore, for each zone and soil type, groups of seven artificial accelerograms fitting the design spectra for 5% damping are generated. The results obtained with these artificial inputs are compared with those for some available historical accelerograms

recorded in Colombia. The sensitivity of the calculated modification factors to the soil type, period and seismic zone is investigated, and matching expressions are generated; such equations are intended to be incorporated into the Colombian regulations. These expressions are compared with previous researches and with the prescriptions of major worldwide design codes; a reasonable fit is observed. Finally, a verification example on a hospital building with seismic isolation and located in Cali (Colombia) is presented and discussed. This example further endorses the proposed approach, since their results are satisfactorily compared with those using the historical records that were employed in the seismic microzonation of Cali.

2 DAMPING MODIFICATION FACTORS

2.1 Concept of design spectrum

The design spectra, although routinely considered for structures described with MDOF models, are derived for linear SDOF systems. The horizontal axis represents the system natural period; the vertical axis displays either displacement, energy (in terms of equivalent velocity) or acceleration. For a given location, the code design spectra are smoothed envelopes of the individual spectra corresponding to a representative suite of accelerograms. The linear equation of motion of a SDOF system under seismic excitation can be written as:

$$m\,\ddot{x} + c\,\dot{x} + k\,x = -m\,\ddot{x}_{\mathrm{g}} \tag{1}$$

In equation (1), m, c and k are mass, damping and stiffness coefficients, x_{g} is the input soil displacement, and x is the output relative displacement, being linked to the absolute displacement (y) by the kinematic relation $x = y - x_{\mathrm{g}}$. The system is mainly characterized by its undamped natural frequency ($\omega = \sqrt{\frac{k}{m}}$) and damping ratio ($\zeta = \frac{c}{2\sqrt{k\,m}}$). The solution of equation (1) is

$$x = -\frac{1}{\omega_{\mathrm{d}}}\int_0^t \ddot{x}_{\mathrm{g}}(\tau)\,\sin\omega_{\mathrm{d}}(t-\tau)\,e^{-\zeta\,\omega\,(t-\tau)}\,d\tau \tag{2}$$

$$\dot{x} = -\int_0^t \ddot{x}_{\mathrm{g}}(\tau)\,\cos\omega_{\mathrm{d}}(t-\tau)\,e^{-\zeta\,\omega\,(t-\tau)}\,d\tau + \frac{\zeta}{\left(1-\zeta^2\right)^{½}}\int_0^t \ddot{x}_{\mathrm{g}}(\tau)\,\sin\omega_{\mathrm{d}}(t-\tau)\,e^{-\zeta\,\omega\,(t-\tau)}\,d\tau \tag{3}$$

$$\ddot{y} = -2\,\zeta\,\omega\,\dot{x} - \omega^2\,x =$$
$$= 2\,\zeta\,\omega\int_0^t \ddot{x}_{\mathrm{g}}(\tau)\,\cos\omega_{\mathrm{d}}(t-\tau)\,e^{-\zeta\,\omega\,(t-\tau)}\,d\tau + \frac{1-2\,\zeta^2}{\left(1-\zeta^2\right)^{½}}\omega\int_0^t \ddot{x}_{\mathrm{g}}\,\sin\omega_{\mathrm{d}}(t-\tau)\,e^{-\zeta\,\omega\,(t-\tau)}\,d\tau \tag{4}$$

In equations (2) through (4), ω_{d} is the damped natural frequency given by $\omega_{\mathrm{d}} = \omega\left(1-\zeta^2\right)^{½}$. The following three response spectra are defined:

$$S_{\mathrm{d}}(\zeta,T) = |x(\zeta,T)|_{\max} \qquad S_{\mathrm{v}}(\zeta,T) = |\dot{x}(\zeta,T)|_{\max} \qquad S_{\mathrm{a}}(\zeta,T) = |\ddot{y}(\zeta,T)|_{\max} \tag{5}$$

S_{d}, S_{v} and S_{a}, are termed as relative displacement, relative velocity, and absolute acceleration response spectra, respectively. By neglecting the difference between the integrals with sinus and cosinus and assuming that ζ is small, in equation (3) $|\dot{x}|_{\max} \approx \omega\,|x|_{\max}$. Analogously, in equation (4) $|\ddot{y}|_{\max} \approx \omega^2\,|x|_{\max}$. Thus, the pseudo-velocity (PS_{v}) and pseudo-acceleration (PS_{a}) response spectra are proposed as:

$$PS_{\mathrm{v}}(\zeta,T) = \omega\,S_{\mathrm{d}}(\zeta,T) \qquad PS_{\mathrm{a}}(\zeta,T) = \omega^2\,S_{\mathrm{d}}(\zeta,T) \tag{6}$$

In force-based design, PS_{a} is the most meaningful, since provides the equivalent static forces that generate the same maximum relative displacement than the accelerogram; thus, reports on structural damage. The design codes contain a smoothed envelope of the corresponding individual spectra, commonly termed as “response acceleration design spectrum”, despite being actually a pseudo-

acceleration spectrum. S_a represents the maximum absolute acceleration, thus reporting on non-structural damage. In displacement-based design [Priestly et al. 2007], displacement spectra (S_d) are considered. These considerations hold even if ζ is not small. Indeed, if ζ is high, the only relevant change is that PS_a and S_a might differ significantly.

For multi-story base isolated buildings, [Kelly 1999] shows that excessive additional damping reduces the displacement at the isolation layer, but at the expense of increasing floor accelerations and interstory drifts in the superstructure. This consideration further emphasizes the need of considering not only S_d, but also S_a. Noticeably, this circumstance cannot be completely derived after the spectra, since they merely correspond to SDOF systems.

2.2 State-of-the-art of research on damping modification factors

A considerable number of studies on the derivation of damping modification factors have been published; only the researches that have most influenced this work are reported herein [Lin, Chang 2003, 2004; Atkinson, Pierre 2004; Lin et al. 2005; Bommer, Mendis 2005; Cameron, Green 2007; Stafford et al. 2008; Casarotti et al. 2009; Cardone et al. 2009; Hatzigeorgiou 2010; Hao et al. 2011; Sheikh et al. 2013; Rezeian et al. 2014; Bradley 2015; Mollaioli et al. 2014; Mavroeidis 2015; Benahmed et al. 2016; Pu et al. 2016; Palermo et al. 2016]. These works examine the influence of a number of issues: fundamental period of the construction, input duration, distance from the site to the hypocenter, magnitude of the earthquake, soil type, forward-directivity effect (near-fault), among others. The following general remarks spring from these studies:

- **Period**. For zero period, the stiffness is infinite; therefore, the relative displacement (x) is null, and the absolute acceleration ($\ddot{y}$) equals the one of the ground. Since both verifications hold for any damping value, it is obvious that the damping modification factors for S_d and S_a are equal to 1 for $T = 0$. At the other end of the spectrum, if T approaches infinite while the damping ratio is maintained constant, the stiffness (k) and damping (c) coefficients approach zero; therefore, the system becomes totally uncoupled from the ground, thus, the relative displacement equals minus the one of the ground, and the absolute acceleration is null. Given that both verifications hold regardless of damping, the damping modification factors for S_d and S_a, also tend to 1 when T tends to infinity. In the short periods range, the damping modification factors become rather extreme, that is, greater/smaller for damping ratios smaller/greater than 5%. Then, for periods ranging approximately between 0.25 s and 1 s, both factors tend to stabilize. Finally, for longer periods, the damping effect decreases slowly but consistently; as discussed previously, the damping modification factors approach one as the period tends to infinity.
- **Input duration**. Differences among response spectra for different damping levels should be greatest for long-lasting excitations, since have more time to develop stationary response, and, thus, fully undergo the damping effect. In other words, the longer the input, the more complete the damping effect. Therefore, the damping modification factors should be significantly more extreme for prolonged accelerograms. [Stafford et al. 2008] shows that the Trifunac duration [Trifunac, Brady 1975] is better correlated to such factors than the number of cycles.
- **Hypocentral distance**. For a given earthquake, apart from local effects, the duration of the inputs grows with the distance between the location and the hypocenter. Thus, as concluded in the previous paragraph, the damping effect increases consistently as that distance grows; hence, the damping modification factor tends to be more extreme.
- **Earthquake magnitude**. Given that events with higher moment magnitude tend to generate records lasting longer, the damping effect is expected to increase accordingly, as concluded when discussing the influence of the input duration. However, this trend is well-established only for periods greater than approximately 0.5 s; for shorter periods this tendency can be inverted.
- **Soil type**. Regarding the influence of soil type, two opposite trends collide: in rock and stiff soil the soil damping is rather low and, therefore, the role of the structural damping is more relevant, but the inputs tend to be shorter. In softer soils, the opposite happens. As a result, the balance is unclear.

- **Near-fault effects**. For pulse-like records, the damping modification factor is, in general, slightly closer to 1 (i.e. less extreme) than for ordinary inputs. This circumstance can be explained by the short duration of such inputs and, more specifically, by the shorter duration of the pulses, being their most destructive part. However, this trend can be inverted for periods close to the pulse period, given that the paramount importance of damping in the response peak.

These remarks highlight the need of considering the influence of period, input duration (and indirectly, hypocentral distance and earthquake magnitude), soil type and near-fault effects in the derivation of damping modification factors for any area.

2.3 Existing methodologies for determining damping modification factors for a given area

All the proposed methodologies are based on calculating, through time-history analyses, the effects of damping on the maximum displacement response of SDOF systems subjected to recorded accelerograms or, less frequently, to artificial ones. Then, the damping modification factor is defined as the ratio between the spectral ordinates (either PS_a or S_d) for the considered value of damping and for 5% damping ($S_d(\zeta,T)$ / $S_d(0.05,T)$). A number of papers [Lin et al. 2005; Cardone et al. 2009; Casarotti et al. 2009; Sheikh et al. 2013] describe comprehensibly the state-of-the-art, including the earliest studies; in view of that, this subsection discusses only the latest researches.

- **Sáez et al. 2012**. Among other contributions, this study proposes, for Chile, an empirical expression of damping reduction factor for different spectral ordinates. This equation is similar to the one proposed in [Lin, Chang 2004], being dependent on period and damping ratio. This expression has been derived after linear dynamic analyses on SDOF systems under 28 scaled Chilean seismic records; these inputs are grouped into hard, intermediate and soft soil. The used scaling procedure is described in [Kottke, Rathje 2008]. The influence of the earthquake type (inter-plate and intra-plate), soil type, and duration of motion is discussed. The obtained factor has been proposed for implementation in the Chilean design code [NCh2745 2013].
- **Anbazhagan et al. 2016**. This work proposes, for the Himalayan Region, damping reduction factors for pseudo-acceleration spectra obtained after local inputs. The main output is an empirical equation for the damping reduction factor in terms of period, moment magnitude, hypocentral distance, and site classification. The authors state that, although the influence of the input duration is significant, it is indirectly represented by the other considered parameters.
- **Mendo, Fernandez-Dávila 2017**. Among other contributions, this study proposes a slight modification, for Peru, of the empirical expression of damping reduction factor originally proposed for Chile [Sáez et al. 2012; NCh 2745 2013]. This expression depends on period and damping ratio, and has been derived after linear dynamic analyses on SDOF systems under 14 two-component Peruvian seismic records; these inputs are grouped into rock and intermediate soil. The obtained factors are in between those of [ASCE 7-10 2010] and [NCh2745 2013].

3 PROPOSED METHODOLOGY FOR DETERMINING DAMPING MODIFICATION FACTORS

The proposed methodology is based on [Sáez et al. 2012]. That research provides damping modification factors for Chilean buildings equipped with energy dissipators; in this work, such approach is extended to any construction with damping ratios differing from 5%. As well, a methodology to compensate the lack of sufficient seismic information is designed.

This work considers two modification factors (termed as B_a and B_d) intended to multiply the corresponding 5% damping design spectrum; B_a and B_d are generated from acceleration and displacement (or pseudo-acceleration) response spectra, respectively:

$$B_a(\zeta,T)=\frac{S_a(\zeta,T)}{S_a(0.05,T)} \qquad B_d(\zeta,T)=\frac{S_d(\zeta,T)}{S_d(0.05,T)}=\frac{PS_a(\zeta,T)}{PS_a(0.05,T)} \tag{7}$$

After the discussion in subsection 2.1, it follows that B_a factor is meant to be used for S_a spectra, thus reporting on non-structural damage. Noticeably, such spectra are not readily available in the design codes; moreover, equation (4) shows that, for high damping ratios and short periods, differences between S_a and PS_a can be considerable. Regarding B_d factor, is meant for both S_d and PS_a spectra, thus reporting on structural damage. Concerning B_v factor (derived after velocity spectra), it is not considered highly meaningful, since S_v does not represent adequately neither input nor hysteretic energy spectra in terms of equivalent velocity [Benavent Climent et al. 2002, 2010; López Almansa et al. 2013].

The most recent studies for determining damping modification factors for a given country or region have been carried out for Taiwan [Lin 2007], Chile [Sáez et al. 2012], the Himalayan region [Anbazhagan et al. 2016] and Perú [Mendo, Fernandez-Dávila 2017]. Some of these investigations have been conducted after scaled accelerograms obtained from locally-recorded actual ground motions. Although this strategy is considered basically correct, it requires a wide set of registers that represent the actual seismicity; if locally-recorded accelerograms are to be used, it is limited to zones with high seismicity (to ensure a sufficient number of strong ground motions), with deeply-studied tectonic mechanisms, and holding a dense, long-standing and reliable seismological network. In developing countries or in areas with moderate or medium seismicity, these conditions are not commonly fulfilled; this work investigates whether the lack of available historical accelerograms can be partly compensated with artificial inputs that are generated to fit the code design spectra. The proposed approach consists in deriving the damping modification factors after a combination of natural and artificial accelerograms. If the artificial inputs are generated for all the design spectra that correspond to each soil type and seismic zone that are specified in the code, they will easily become more numerous and representative than the available historical accelerograms; therefore, the proposed strategy consists in deriving initially the damping modification factors after the artificial accelerograms, and then comparing with the recorded ones for further verification and refining.

This strategy releases, to some extent, the need of taking into consideration the magnitude of the earthquake and the hypocentral distance, since these issues are implicitly incorporated in the design spectra for each seismic zone the country is divided in. Conversely, the research [Stafford et al. 2008] has pointed out that the differences between the numbers of cycles of recorded and artificial accelerograms might lead to significant discrepancies among the damping modification factors derived after them; therefore, the generation of duration-compatible artificial inputs needs to be seriously taken this consideration.

Noticeably, the proposed strategy is considered particularly suitable for determination of damping modification factors for relatively small and highly populated urban areas where microzonation studies have been carried out, given that typically only few records are readily available.

4 STUDY FOR COLOMBIA

4.1 General description

Given the aforementioned scarcity of seismic records in Colombia, the study is mainly based on artificial inputs. Initially, fifty groups of seven artificial accelerograms are generated; each group corresponds to a given seismic zone in Colombia (ten zones, [NSR-10 2010]) and a given soil type (five types, A through E, [NSR-10 2010]). The inputs are created to match the 5% damping design response acceleration spectra for the corresponding seismic zone and soil type. For each accelerogram, linear dynamic analyses are conducted on SDOF systems; their natural period (T) and damping ratio (ζ) range between 0.01 and 4 s, and 0.005 (0.5%) and 0.5 (50%), respectively. In each case (for a given seismic zone, soil type, and damping ratio) the seven obtained pairs of individual S_d and S_a spectra are averaged. Then, the modification factors B_d and B_a are defined as indicated in equation (7). The obtained results are compared with the most relevant available accelerograms recorded in Colombia.

Nineteen values of damping ratio ranging between 0.005 and 0.5 are considered: 0.005, 0.01, 0.015, 0.02, 0.025, 0.03, 0.035, 0.04, 0.045, 0.05, 0.1, 0.15, 0.20, 0.25, 0.3, 0.35, 0.4, 0.45 and 0.5. Regarding the period, 3990 values are taken, ranging from 0.01 and 4 s. Therefore, for the artificial inputs, the number of conducted dynamic analyses is: 10 (zones) × 5 (soil types) × 7 (accelerograms) × 19 (damping ratios) × 3990 (natural periods) = 26,533,500. As well, additional analyses are performed to provide sounder basis for the derived conclusions; among them, calculations for damping ratios in the range between 0.5 and 0.8.

In each dynamic analysis, the solution of equation (1) is obtained as indicated in equations (2) through (4); the involved Duhamel integrals are solved numerically by assuming linear interpolation of acceleration. For systems with natural period longer than 0.04 s, the time step is 0.01 s; for systems with shorter periods, the time step is selected as $T / 4$.

4.2 Design spectra for Colombia

As discussed in the previous subsection, the Colombian code [NSR-10 2010] divides the country in ten seismic zones, being numbered as 1 (lowest seismicity) through 10 (highest seismicity). Regarding the soil classification, it follows basically the American regulation [ASCE 7-10 2010]; six categories are considered, ranging from A (hard rock, average shear wave velocity higher or equal than 1500 m/s) through F. Given that soil type F routinely requires particular studies, and that no design spectra are provided in the code, only types A through E (average shear wave velocity lower than 180 m/s) are considered in this study. Fifty design spectra are generated, corresponding to the ten seismic zones and the five major soil types.

The seismic zones are classified with respect to the parameter A_a, which represents the design PGA (spectral ordinate zero-period) in soil type A [NSR-10 2010]. The site seismicity is also characterized by the parameter A_v, which affects the medium and long period ranges of the spectrum; noticeably, the divisions of the country in seismic zones according to both parameters are not always coincident. Each zone is represented by a city having maximum values of A_a and A_v. Table 1 describes the main characteristics of the considered zones. Table 1 highlights the extreme discrepancies among the zones, ranging from low seismicity in zone 1 to high one in zone 10.

The spectra are generated by assuming that the importance (I) and response modification (R) factors are equal to one. The obtained spectral ordinates are intended to multiply the building seismic weight to provide the base shear force; such ordinates are termed S_a in the Colombian code, although they actually correspond to PS_a (pseudo-acceleration spectra). Each spectrum is composed of three branches: constant acceleration (short periods), constant velocity (intermediate periods) and constant displacement (long periods); the boundaries between these intervals are termed T_C and T_L, respectively. Table 2 displays the values of T_C and T_L for each zone and soil type.

Table 1. Considered seismic zones

Zone	**Representative city**	**A_a (g)**	**A_v (g)**
1	Leticia	0.05	0.05
2	Valledupar	0.10	0.10
3	Arauca	0.15	0.15
4	Tunja	0.20	0.20
5	Manizales	0.25	0.25
6	El Carmen de Atrato	0.30	0.30
7	Quibdó	0.35	0.35
8	Alto Baudo	0.40	0.40
9	Tumaco	0.45	0.40
10	Olaya Herrera	0.50	0.40

Table 2. T_C / T_L periods (s) in the Colombian code

Soil type	**Zone**									
	1	2	3	4	5	6	7	8	9	10
A	0.48/1.92	0.48/1.92	0.48/1.92	0.48/1.92	0.48/1.92	0.48/1.92	0.48/1.92	0.48/1.92	0.43/1.92	0.38/1.92
B	0.48/2.40	0.48/2.40	0.48/2.40	0.48/2.40	0.48/2.40	0.48/2.40	0.48/2.40	0.48/2.40	0.43/2.40	0.38/2.40
C	0.68/4.08	0.68/4.08	0.66/3.96	0.64/3.84	0.65/3.72	0.66/3.60	0.66/3.48	0.67/3.36	0.60/3.36	0.54/3.36
D	0.72/5.76	0.72/5.76	0.70/5.28	0.69/4.80	0.70/4.56	0.72/4.32	0.71/4.08	0.70/3.84	0.65/3.84	0.61/3.84
E	0.67/8.40	0.67/8.40	0.77/8.04	0.90/7.68	0.99/7.20	1.12/6.72	1.19/6.24	1.28/5.76	1.14/5.76	1.02/5.76

Figure 1 displays the pseudo-acceleration design spectra for each seismic zone and soil type. Figure 1.a through Figure 1.e contain sets of ten spectra (for each zone) corresponding to soils A through E, respectively. For the sake of further comparison, Figure 1.f presents, for zone 10, five spectra corresponding to each soil type, respectively. Figure 1.f shows that the softest soil (type E) does not always hold the highest spectral ordinates for the whole range of periods. Noticeably, the Colombian design spectra contain also an inclined initial branch; such segment is not included here, given that it is only intended for spectral analyses for the higher modes.

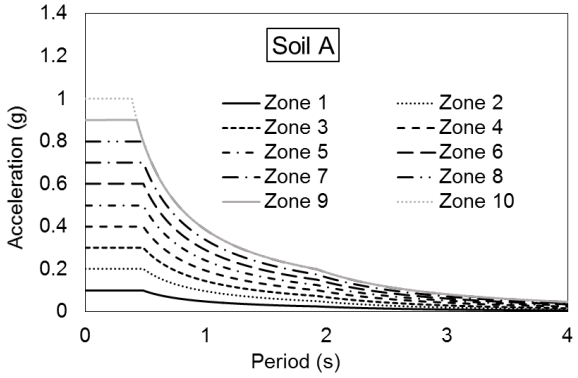

(a) Pseudo-acceleration spectra for soil type A

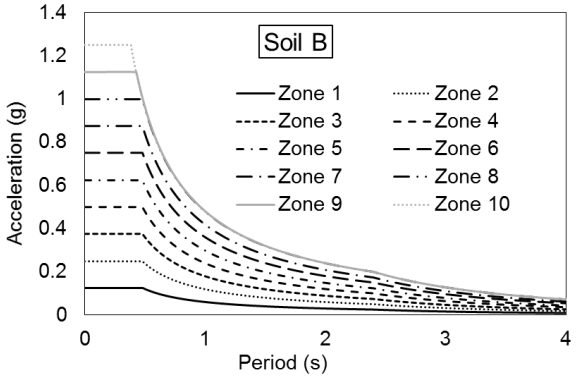

(b) Pseudo-acceleration spectra for soil type B

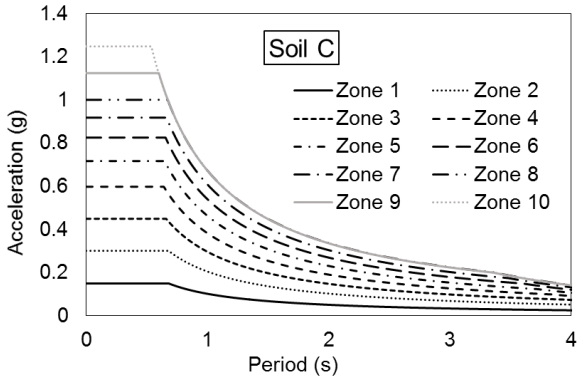

(c) Pseudo-acceleration spectra for soil type C

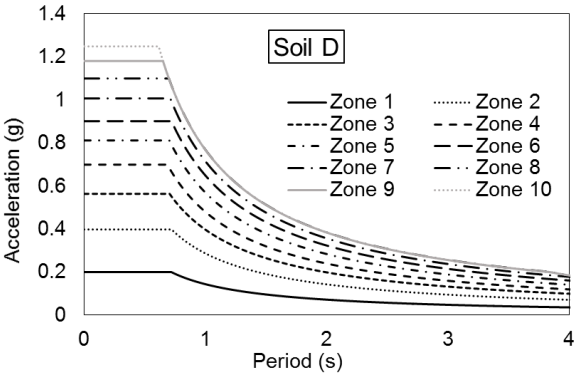

(d) Pseudo-acceleration spectra for soil type D

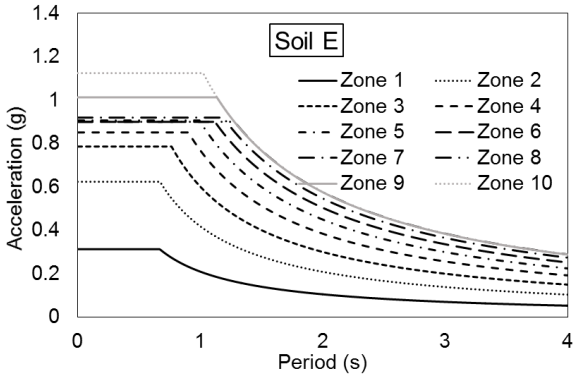

(e) Pseudo-acceleration spectra for soil type E

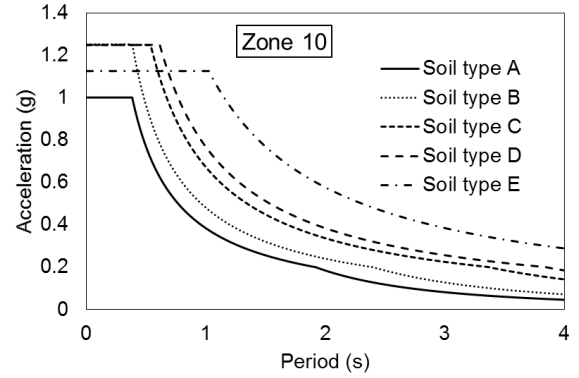

(f) Pseudo-acceleration spectra for zone 10

Figure 1. Design spectra in the Colombian design code [NSR-10 2010]

The plots from Figure 1.a through Figure 1.e show that, for each soil type, the spectra for the ten zones are approximately homothetic, namely vertically scaled with the A_a coefficient (Table 1). Therefore, given that the artificial inputs are generated to fit these spectra, the inputs for the ten zones that correspond to a given soil type will be also approximately homothetic; therefore, since the damping

modification factors are obtained after linear analyses, no big differences among the ten zones are to be expected.

4.3 Artificial seismic inputs

As discussed in section 1, fifty groups of artificial accelerograms are created; each group has seven accelerograms. These groups correspond to the ten seismic zones in Colombia (1–10) and the five soil types (A–E) that have been considered. The number of accelerograms inside each group has been set as seven, as indicated by [ASCE 7-10 2010; ASCE 7-16 2016] for base-isolated buildings. The accelerograms are created to match the 5% damping acceleration design response spectrum by using the SeismoArtif software [Seismosoft 2016]. The inputs are generated for 20 s duration, as their Trifunac duration [Trifunac, Brady 1975] matches those of the available local records (section 5). The variation of amplitude vs. time responds to the random function described in [Saragoni, Hart 1973], by selecting that the maximum amplitude corresponds to 4 s and the final instant amplitude is 5% of the maximum one. The choice of the function in [Saragoni, Hart 1973] is based on its superior capacity to reproduce the behavior of actual inputs; the parameters are selected by accounting for the aforementioned high sensitivity of the damping modification factor to the input duration. The quadratic error and coefficient of variation (averaged for the 350 accelerograms) are 8.70% and 0.0997, respectively; the discretization period is 0.01 s. Figure 2.a displays an example of a sample accelerogram whose response spectrum fits the design spectrum of the Colombian code [Piscal A. 2018]; Figure 2.b presents comparison among such design spectrum and those of the seven corresponding artificial accelerograms (one of them is displayed in Figure 2.a).

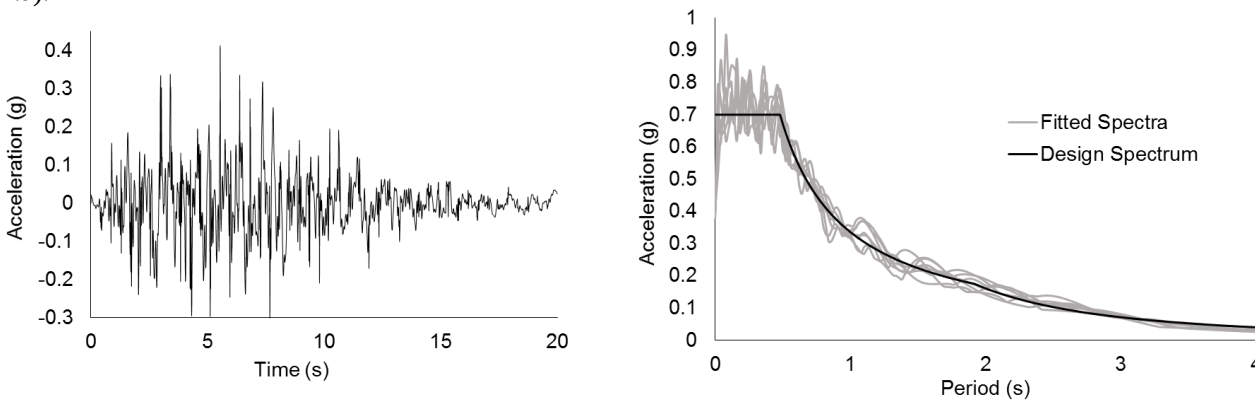

(a) Sample artificial accelerogram (b) Individual spectra and design spectrum

Figure 2. Accelerograms selected to fit a design spectrum for zone 7 and soil type A

Figure 2.b highlights the great similarity between the target code design spectrum and the individual response spectra of the generated artificial accelerograms.

4.4 Obtained results

Figure 3 displays sample spectra for factors B_d (Figure 3.a) and B_a (Figure 3.b); the selected case corresponds to Zone 7, soil type A and damping 30%. Each figure presents seven plots of B_d or B_a vs. period corresponding to seven individual accelerograms, and their average spectrum; noticeably, apparently, only 6 individual spectra can be observed because two of them are almost coincident. Figure 3 shows that the dispersion of the seven spectra that correspond to the same design spectrum (i.e. same seismic zone and soil type) is rather moderate.

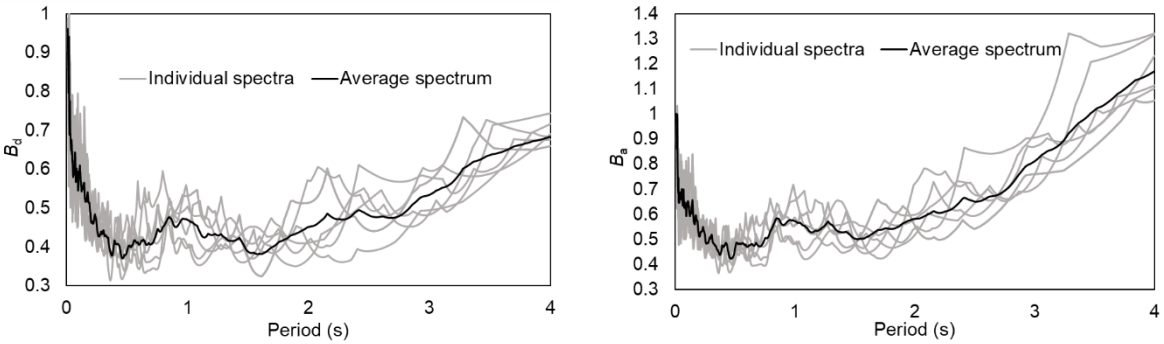

(a) B_d factor (b) B_a factor

Figure 3. Sample spectra for factor B_d and B_a for seven artificial accelerograms. Zone 7, soil A and damping 30%

The observation of the results averaged for each group (of seven accelerograms) shows little influence of the seismic zone (subsection 4.2) [Piscal A. 2018], this being coherent with the complexity of the tectonics of Colombia; therefore, the values of B_d and B_a are averaged for the ten zones. Thus, Figure 4 displays plots of factors B_d vs. period for each soil type and some representative values of the damping ratio (0.005, 0.01, 0.02, 0.04, 0.07, 0.10, 0.20 and 0.30); Figure 4.a through Figure 4.e contain plots of B_d for the soil types A through E, respectively. The observation of these plots shows also little influence of the soil type. Hence, Figure 4.f presents plots of B_d averaged for all the soil types. Figure 5 displays similar plots of the factor B_a.

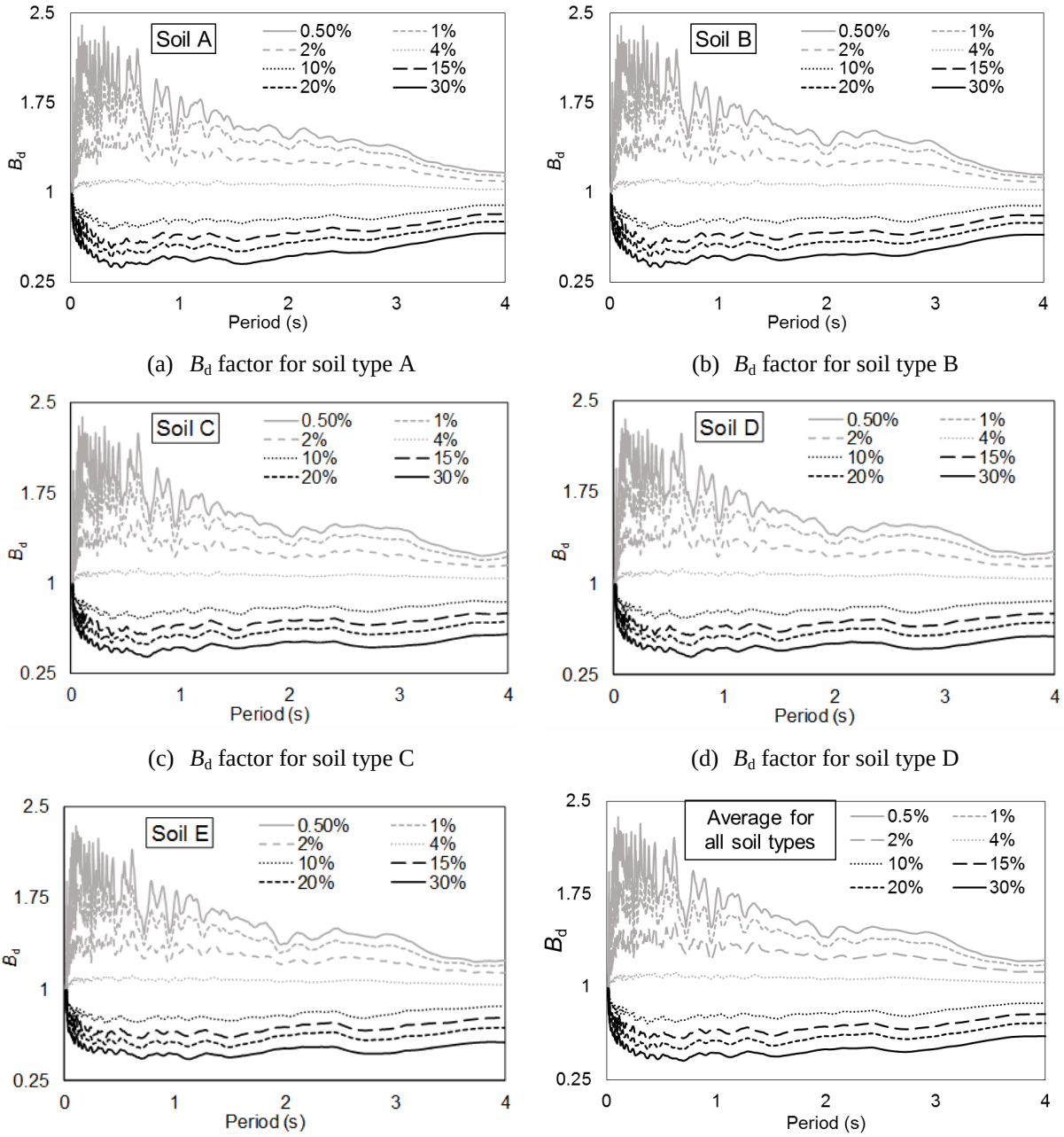

(a) B_d factor for soil type A

(b) B_d factor for soil type B

(c) B_d factor for soil type C

(d) B_d factor for soil type D

(e) B_d factor for soil type E

(f) B_d factor for all soil types

Figure 4. Spectra for factor B_d

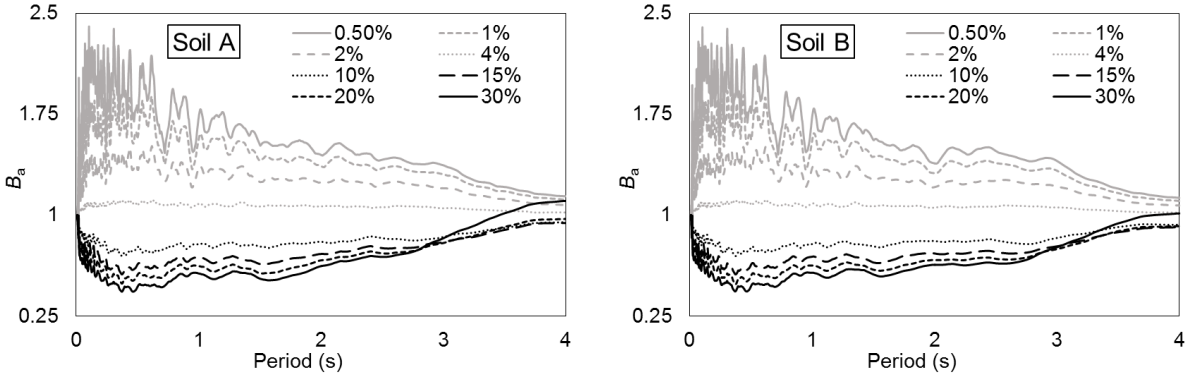

(a) B_a factor for soil type A

(b) B_a factor for soil type B

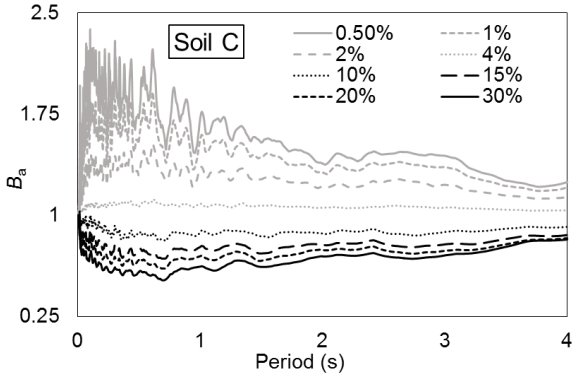

(c) B_a factor for soil type C

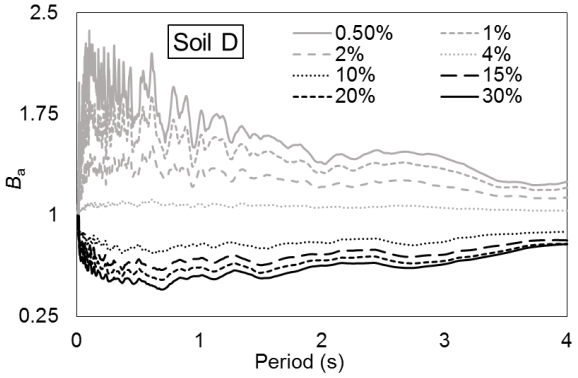

(d) B_a factor for soil type D

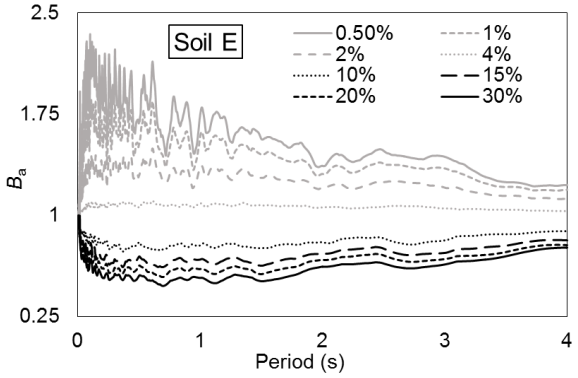

(e) B_a factor for soil type E

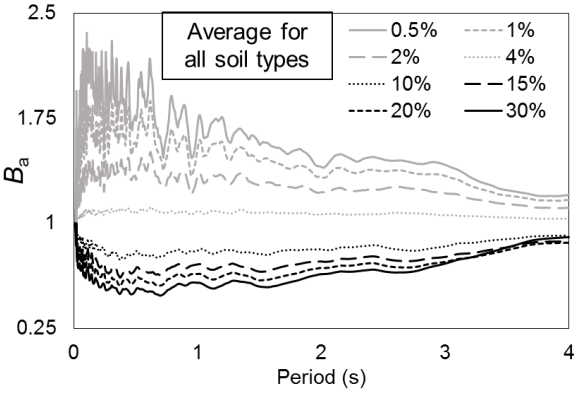

(f) B_a factor for all soil types

Figure 5. Spectra for factor B_a

Figure 4 and Figure 5 show regular behavior, with results fitting basically the previous studies (subsection 2.2). Noticeably, for short periods and low damping, the dispersion is high.

4.5 Derived expressions for B_d and B_a factors

This subsection describes the genesis of the recommended fitting expressions for B_d and B_a factors. These relations are derived to match the plots in Figure 4.f and Figure 5.f, respectively. The starting points are the criteria provided for B_d and B_a in [Lin, Chang 2004]. For B_d, this work considers the expression $B_d = 1 - \frac{a\,T^b}{(T+1)^c}$, where the coefficient a contains the influence of damping and $\frac{T^b}{(T+1)^c}$ represents the effect of period; the selected values and expressions are b = 0.3, c = 0.65 and a = 1.3033 + 0.436 ln ζ. For B_a, $B_a = d + e\,T$; for T > 0.2 s, d = 0.342 $\zeta^{-0.354}$ and e = 0.0186 + 0.368 (ζ − 1) /

10.644 ζ^2, and for $T < 0.2$ s, a linear interpolation starting from $B_a = 1$ for $T = 0$ s (subsection 2.2), is suggested. The investigation [Lin, Chang 2004] refers only to damping ratios greater than 5%; conversely, the spectra in Figure 4.f and Figure 5.f include also damping ratios smaller than 5%. The derivation of the matching expressions is described next for both cases.

Damping ratio higher than 5%. For B_d, the same expression proposed in [Lin, Chang 2004] ($B_d = 1 - \frac{a\,T^b}{(T+1)^c}$) is considered. The process starts by selecting the values of the coefficients *a*, *b* and *c* that better fit the spectra in Figure 4.f for damping ratio 30%; this operation is performed by nonlinear regression using the damped least-squares (Levenberg-Marquardt) algorithm implemented in Gnuplot [Williams, Kelley 2011]. For damping ratios 50%, 45%, 40%, 35%, 25%, 20%, 15% and 10%, the values of coefficients *b* and *c* are kept constant, while *a* is obtained with the same algorithm. For B_a, a trilinear fit is suggested; the coefficients of each linear segment ($B_a = d + e\,T$) are determined by linear regression. Table 3 displays the obtained values of the coefficients *a*, *b* and *c* (B_d) and *d* and *e* (B_a).

Table 3. Coefficients of the derived expressions for B_d and B_a for damping ratio higher than 5%

Damping ratio	$B_d = 1 - \frac{a\,T^b}{(T+1)^c}$			$B_a = d + e\,T$					
				$T \le 0.04$ s		0.04 s < $T \le 0.5$ s		0.5 s < $T \le 4$ s	
	a	*b*	*c*	*d*	*e*	*d*	*e*	*d*	*e*
0.50	1.249	0.3683	0.9200	1.000	– 10.70	0.5873	– 0.3778	0.3184	0.1679
0.45	1.211	0.3683	0.9200	1.000	– 10.27	0.6047	– 0.3880	0.3368	0.1524
0.40	1.166	0.3683	0.9200	1.000	– 9.79	0.6241	– 0.3996	0.3585	0.1368
0.35	1.112	0.3683	0.9200	1.000	– 9.25	0.6461	– 0.3991	0.3849	0.1213
0.30	1.045	0.3683	0.9200	1.000	– 8,61	0.6716	– 0.3954	0.4178	0.1058
0.25	0.9603	0.3683	0.9200	1.000	– 7.84	0.7016	– 0.3846	0.4604	0.0903
0.20	0.8487	0.3683	0.9200	1.000	– 6.90	0.7385	– 0.3597	0.5184	0.0747
0.15	0.6912	0.3683	0.9200	1.000	– 5.65	0.7859	– 0.3027	0.6041	0.0592
0.10	0.4493	0.3683	0.9200	1.000	– 3.86	0.8528	– 0.1788	0.7496	0.0437

Damping ratio lower than 5%. For both B_d and B_a, the same expression proposed in [Lin, Chang 2004] for B_d ($B_d = 1 - \frac{a\,T^b}{(T+1)^c}$) is considered. For B_d, the process starts by selecting the values of the coefficients *a*, *b* and *c* that better fit the spectra in Figure 4.f for damping ratio 4%; this operation is performed by nonlinear regression using the damped least-squares (Levenberg-Marquardt) algorithm implemented in Gnuplot [Williams, Kelley 2011]. For damping ratios 5%, 3%, 2.5%, 2%, 1.5%, 1% and 0.5% the coefficient *b* remains constant, while *a* and *c* are obtained with the same algorithm. For B_a, the process is analogous, although none coefficient remains constant for any damping ratio. Table 4 displays the obtained values of the coefficients *a*, *b* and *c*.

Table 4. Coefficients of the derived expression for B_d and B_a for damping ratio lower than 5%

Damping ratio	$B_d = 1 - \frac{a\,T^b}{(T+1)^c}$			$B_a = 1 - \frac{a\,T^b}{(T+1)^c}$		
	a	*b*	*c*	*a*	*b*	*c*
0.040	– 0.2220	0.4685	1.399	– 0.2449	0.4942	1.4673
0.035	– 0.3632	0.4685	1.432	– 0.3591	0.4828	1.4859
0.030	– 0.5340	0.4685	1.472	– 0.5179	0.4749	1.5022
0.025	– 0.7463	0.4685	1.522	– 0.7211	0.4649	1.5189
0.020	– 1.017	0.4685	1.580	– 0.9689	0.4471	1.5346
0.015	– 1.378	0.4685	1.653	– 1.2611	0.4157	1.5438
0.010	– 1.905	0.4685	1.754	– 1.5979	0.3652	1.5366
0.005	– 2.815	0.4685	1.918	– 1.9792	0.2898	1.4993

Figure 6 displays comparisons among the spectra represented in Figure 4.f and Figure 5.f and the fittings given by the expressions $1 - \frac{a\,T^b}{(T+1)^c}$, and $d + e\,T$, where the coefficients *a*, *b*, *c*, *d* and *e* are given in Table 3 and Table 4.

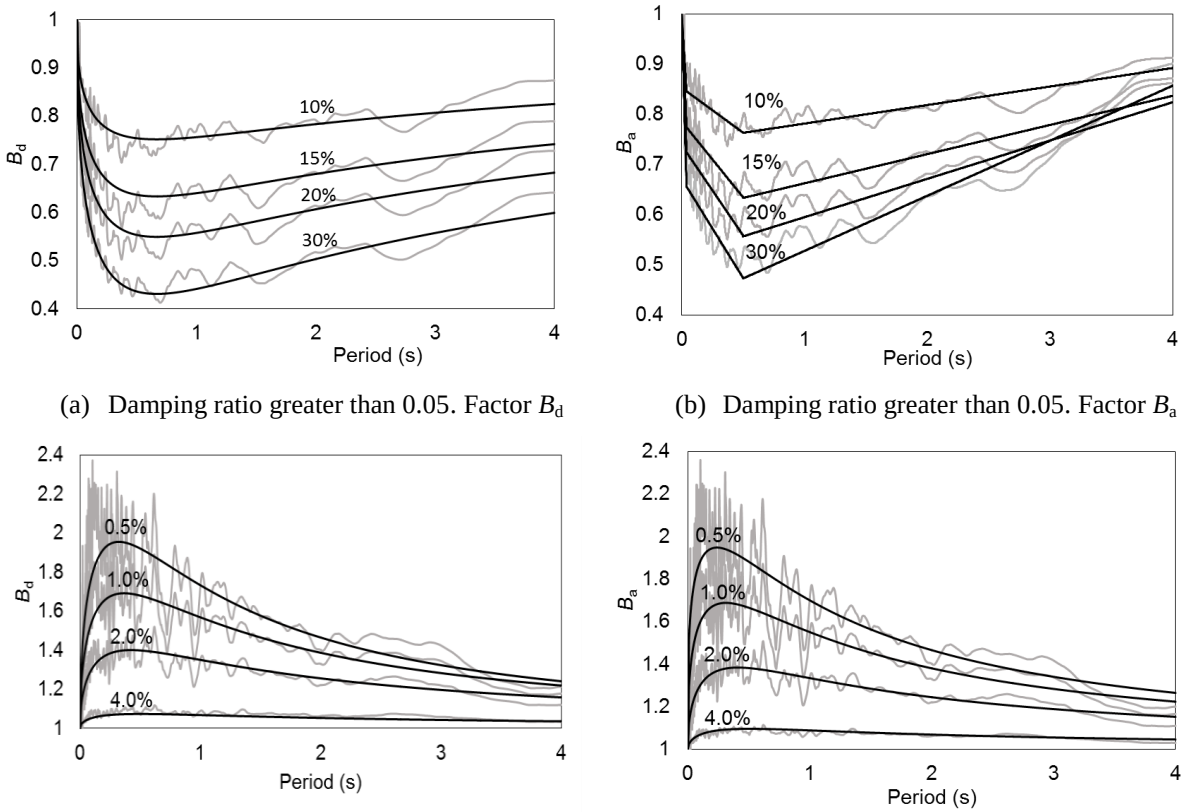

(a) Damping ratio greater than 0.05. Factor B_d

(b) Damping ratio greater than 0.05. Factor B_a

(c) Damping ratio smaller than 0.05. Factor B_d

(d) Damping ratio smaller than 0.05. Factor B_a

Figure 6. Comparison among the obtained spectra for factors B_d and B_a with the derived fits

The plots from Figure 6 confirm that the fits are correct.

The process is completed by generating expressions of the coefficients *a*, *b*, *c*, *d* and *e* in terms of the damping ratio. The derived expressions are summarized in Table 5.

Table 5. Derived expressions for B_d and B_a			
$\zeta > 0.05$ $B_d = 1 - \frac{a\,T^b}{(T+1)^c}$	a		$1.621 + 0.4935 \ln \zeta$
	b		0.3683
	c		0.9200
$\zeta > 0.05$ $B_a = d + e\,T$	$T \leq 0.04$ s	d	1
		e	$-789.9\,\zeta^5 + 1445\,\zeta^4 - 1071\,\zeta^3 + 419.7\,\zeta^2 - 100.6\,\zeta + 2.938$
	0.04 s < $T \leq$ 0.5 s	d	$-0.165 \ln \zeta + 0.4729$
		e	$-139\,\zeta^5 + 248.6\,\zeta^4 - 176.7\,\zeta^3 + 63.64\,\zeta^2 - 11.83\,\zeta + 0.521$
	0.5 s < $T \leq$ 4 s	d	$0.2202\,\zeta^{-0.532}$
		e	$-0.2028\,\zeta^2 + 0.4355\,\zeta - 0.0026$
$\zeta < 0.05$ $B_d = 1 - \frac{a\,T^b}{(T+1)^c}$	a		$3.789 + 1.238 \ln \zeta$
	b		0.4685
	c		$0.5941 - 0.2510 \ln \zeta$
$\zeta < 0.05$ $B_a = 1 - \frac{a\,T^b}{(T+1)^c}$	a		$-890.2\,\zeta^2 + 89.61\,\zeta - 2.405$
	b		$7576\,\zeta^3 - 724.6\,\zeta^2 + 24.62\,\zeta + 0.1839$
	c		$-274530\,\zeta^4 + 32146\,\zeta^3 - 1395\,\zeta^2 + 23.27\,\zeta + 1.414$

5 COMPARISON WITH ACTUAL COLOMBIAN ACCELEROGRAMS

5.1 Initial considerations

This section presents a comparison among the results obtained in the previous section (after artificial accelerograms) with results derived from some available Colombian natural inputs.

5.2 Recorded inputs in Colombia

A number of historical accelerograms recorded in Colombia have been selected; the selection criteria are: local magnitude greater or equal than 6.0, and epicentral distance less than 210 km. This information has been retrieved from the Colombian Seismological National Network [RSNC 2017]; noticeably, the soil type is taken from [Benavent-Climent et al. 2010]. The time step is 0.005 s. For the baseline correction, a constant polynomial is used; then, a 4th order Butterworth filter with a bandpass configuration (0.1-20 Hz) is employed. Given that most of the available relevant records correspond to the zone 5, this study is constrained to that area. Table 6 displays the main characteristics of the selected historical records. The hypocentral distance corresponds to the straight separation between the hypocenter and the recording station. I_A is the Arias Intensity [Arias 1970] given by $I_A = \frac{\pi}{2\,g}\int \ddot{x}_g^2\,dt$, where $\ddot{x}_g$ is the input ground acceleration; I_A is an estimator of the input severity. The Trifunac duration is defined as the time elapsed between the 5% and the 95% of the Arias Intensity [Trifunac, Brady 1975]. The Housner intensity [Housner 1952] is defined as the area enclosed, between 0.1 and 2.5 s, by the 5% damping elastic pseudo-spectral velocity spectrum.

Table 6. Selected Colombian records for seismic zone 5

Soil type	Earthquake epicenter	Date	Local magnitude (M_L)	Hypocentral depth (km)	Station	Epicentral / Hypocentral distance (km)	Component	PGA (cm/s^2)	Arias intensity (cm/s)	Trifunac duration	Housner intensity (cm)
A	Calima	1995/02/08	6.6	102	CTRUJ	47.44 / 112.49	EW	109.36	8.15	17.36	29.21
							NS	93.09	8.11	18.04	22.53
					CSEVI	90.57 / 136.41	EW	80.46	11.67	22.46	9.79
							NS	45.94	4.69	25.60	9.85
	Risaralda	1995/08/19	6.5	120.90	CANSE	18.43 / 122.30	EW	80.93	11.24	24.85	9.35
							NS	166.51	34.15	25.10	9.99
	Córdoba	1999/01/25	6.3	0	CBOCA	38.48 / 38.48	EW	85.76	3.70	6.47	19.04
							NS	52.94	2.33	9.03	12.76
C	Génova	1997/09/02	6.8	230	CARME	69.58 / 240.29	EW	70.61	9.53	37.13	10.53
							NS	60.91	11.85	36.34	11.21
	Génova	1997/12/11	6.5	207.50	CCALI	83.48 / 223.66	EW	46.79	4.14	26.30	11.38
							NS	39.31	3.56	31.76	12.97
					CMAN1	137.10 / 248.70	EW	62.18	7.94	15.77	18.31
							NS	75.42	14.83	15.59	24.77
					CPER2	95.40 / 228.38	EW	46.65	6.39	22.07	12.56
							NS	45.57	6.80	22.68	12.58
	Córdoba	1999/01/25	6.3	0	CMAN1	79.45 / 79.45	EW	85.23	22.08	19.16	33.83
							NS	105.90	23.07	18.16	34.91
					CARME	13.02 / 13.02	EW	517.23	272.89	11.06	88.83
							NS	576.16	278.44	9.54	84.36
	Bajo Baudo	2004/11/15	6.7	26.2	CVERS	169.95 / 171.96	EW	49.76	16.14	50.85	16.28
							NS	47.22	15.61	52.70	16.53
D	Génova	1997/12/11	6.5	207.50	CFLAN	86.32 / 224.74	EW	84.47	16.14	25.54	21.64
							NS	85.15	22.34	28.50	26.79
	Córdoba	1999/01/25	6.3	0	CFLAN	28.85 / 28.85	EW	573.67	296.59	14.32	125.21
							NS	506.67	425.71	10.13	129.84
	Bajo Baudo	2004/11/15	6.7	26.2	CCAL5	197.28 / 199.01	EW	54.70	9.37	35.34	57.10
							NS	31.46	6.02	49.00	40.40
					RAC03	199.16 / 200.88	EW	61.64	16.19	34.24	55.41
							NS	24.74	3.02	40.61	23.00
					RAC06	199.27 / 200.99	EW	79.48	25.32	38.60	88.11
							NS	37.34	6.29	30.21	38.32
					RAC07	195.25 / 197.00	EW	29.66	1.75	27.44	19.54
							NS	20.57	1.10	28.20	20.46
					RAC08	198.62 / 200.34	EW	46.56	11.65	48.69	55.06
							NS	29.31	4.47	37.85	37.69
					RAC10	204.07 / 205.74	EW	67.57	16.00	75.57	59.44
							NS	23.00	4.94	63.52	34.57
					RAC11	207.25 / 208.90	EW	55.26	18.39	66.47	61.79
							NS	25.20	4.62	63.58	32.44

For the sake of comparison with the historical inputs in Table 6, Table 7 displays the average parameters of the suites of seven artificial inputs (subsection 4.3) that correspond to the same seismic zone and soil type. Table 7 shows that the available historical records are significantly less severe than the corresponding artificial ones, except for the four strongest records of the Armenia earthquake (Table 6, Córdoba 1999/01/25 event). Regarding the Trifunac duration [Trifunac, Brady 1975], Table 6 shows that, for such four inputs, it is equal to 11.06, 9.54, 14.32 and 10.13 s; comparison with the values in Table 7 shows a rather satisfactory agreement.

Table 7. Average parameters of the artificial inputs in zone 5

Soil type	PGA (cm/s^2)	Trifunac duration (s)	Arias intensity (cm/s)	Housner intensity (cm)
A	275.89	10.29	82.52	82.68
C	408.01	10.53	207.36	156.07
D	462.58	10.51	276.52	186.32

5.3 Comparison between spectra from artificial and natural accelerograms

Figure 7 displays comparisons among 30%-damped B_d spectra obtained after natural and artificial inputs. Figure 7.a, Figure 7.b and Figure 7.c correspond to soil A, C and D, respectively; each Figure contains three types of plots: those corresponding to the strongest components of the individual records listed in Table 6, their average, and the average of the spectra derived after the artificial inputs that belong to the same seismic zone, damping level (30%) and soil type. Figure 7.d presents a similar comparison referring to the average spectra for soils A, C and D. Figure 7.d. also contains three types of plots: individual for all the records in Table 6, their average, and the corresponding fitted expression that is displayed in Table 3.

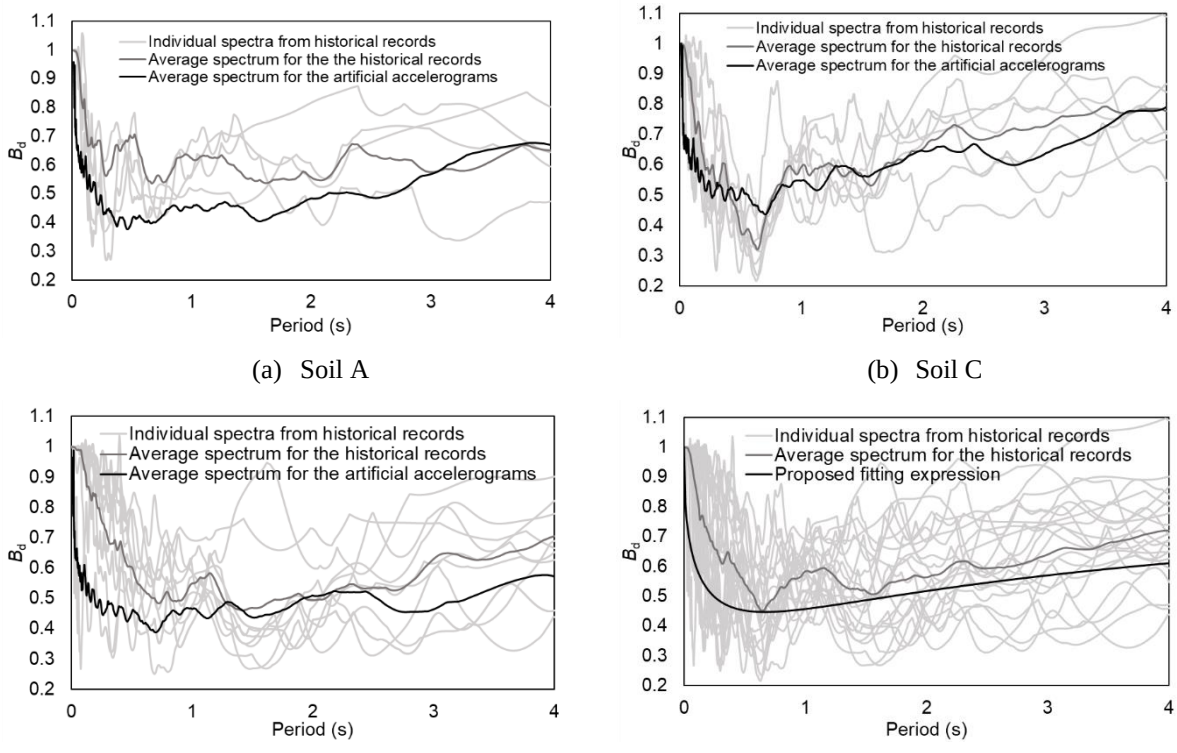

(a) Soil A (b) Soil C

(c) Soil D (d) Average for soil types A, C and D

Figure 7. Comparison between B_d spectra for artificial and historical accelerograms in zone 5 for damping 30%

The plots from Figure 7 show a reasonably satisfactory agreement between the spectra generated from recorded and artificial inputs, given the extreme scarcity and high dispersion exhibited by the B_d spectra for the historical accelerograms. Noticeably, to assess the relevance of the observed

discrepancies between the spectra generated after both types of accelerograms, it should be kept on mind that the available historical inputs are too scarce to be considered representative of the actual seismicity of Colombia.

6 COMPARISON WITH FACTORS DEFINED IN CODES AND IN THE LITERATURE

This section compares the main output of this study (i.e. the matching expression for the B_d that is factor presented in Table 3) with previous proposals, either from reported studies or from design codes. Figure 8 displays a comparison among the expression derived in this study for B_d, and the results of previous researches [Lin 2004; Sáez 2012] and of the codes of Chile [NCh 2745 2013], Japan [BSLEO 2009], USA [ASCE 7/10 2010], Europe [EN-1998 2005] and China [GB50011 2010]. Figure 8.a, Figure 8.b, Figure 8.c, and Figure 8.d present B_d spectra for 30%, 20% 10% and 2% damping ratio, respectively.

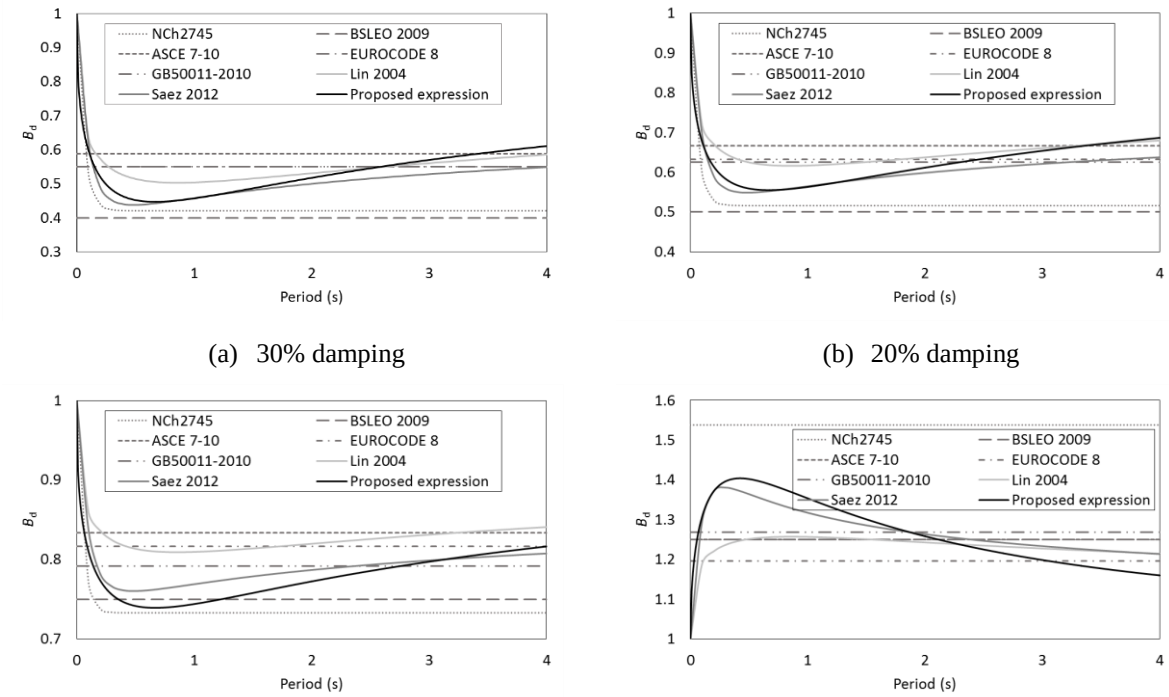

(a) 30% damping (b) 20% damping

(c) 10% damping (d) 2% damping

Figure 8. Comparison among B_d code spectra with the results of this and previous studies

The plots from Figure 8 show that the results of this study fit reasonably well those of the previous researches [Lin 2004; Sáez 2012]. Regarding the design codes, the derived expression lies within their range; noticeably, the analyzed codes show an important scattering.

The current Colombian design code [NSR-10 2010] does not contain any criteria to modify the 5%-damped spectra; for seismic isolation, the USA regulations [ASCE 7/10 2010] are used instead. Figure 8 shows relevant disagreements between that criterion and the results of this study. Such differences can be due to the fact that the US accelerograms have shorter duration and are rather pulse-like [Sáez et al. 2012]. In any case, for the ranges of periods and damping ratios of interest in seismic isolation (period between 2.5 and 3.5 s, and damping ratio between 20% and 30%), Figure 8.a and Figure 8.b show that the discrepancies are significantly smaller.

It is worth noting that the Japanese, European and Chinese codes do not allow further reduction of the spectral ordinates for damping ratios higher than 30%; analogously, in the USA and Chilean regulations, such bound is 50%. This study corroborates this strategy, since, for damping ratios

exceeding approximately 50%, B_a factor can be greater than 1, thus generating an increase of the absolute accelerations [Piscal A. 2018].

7 VERIFICATION EXAMPLE

This section discusses an application example on a 4-story RC base-isolated hospital building located in Cali (Colombia) [Piscal, López Almansa 2016]. This study aims to verify the accuracy of the proposed approach by comparing the maximum design displacement of the isolation layer (D_D) determined with three different approaches: (i) equivalent lateral forces method [ASCE 7-10 2010], (ii) the same method, although considering the derived B_d factor instead, (iii) nonlinear time-history analysis using 7 actual records that had been utilized in the microzonation of Cali [Decreto 158 2014]. A more extended description of this study is available in [Piscal A. 2018].

The building is the 4-story "Clínica Confandi", being the first base-isolated hospital in Colombia. It has a RC framed structure. The plan is rectangular, with sides 50.4 and 17 m, and the seismic weight is 35021 kN. The foundation soil belongs to zone 4D according to the Cali microzonation [Decreto 158 2014], being equivalent to soil D [NSR-10 2010]. A deeper description of this building can be found in [Piscal, López Almansa 2016].

The isolation layer consists of 32 bearings; two types of isolator units are employed: natural rubber bearings (NRB) and lead-rubber bearings (LRB). Three isolation solutions have been investigated; they differ in the characteristics of the isolators and the target values of the fundamental period and the damping ratio of the isolated building. Table 8 displays the main features of the three analyzed solutions.

Table 8. Isolation solutions for the example hospital building

Solution No.	LRB			NRB		Damping ratio (%)	Fundamental period (s)
	No.	Diameter / Height* (mm)	Lead plug diam. (mm)	No.	Diameter / Height* (mm)		
1	20	450 / 96	90	12	450 / 60	16.69	2.15
2	24	400 / 126	78	8	400 / 78	19.76	3.00
3	32	500 / 210	120	-	-	29.84	2.42

*Rubber height (sum of the thickness of each rubber layer)

In the first approach, the isolators displacement is determined after the expression $D_D = \frac{S_a T^2}{4 \pi^2 B}$, where T is the fundamental period of the isolated building in the direction under consideration, S_a is the spectral ordinate corresponding to this period, and B is the reduction factor due to damping. S_a is determined after the corresponding design spectra in the Cali microzonation [Decreto 158 2014], and B = 1.40, 1.49 and 1.70 for solutions 1, 2 and 3, respectively. In the second approach, 1 / B is represented by the derived coefficient B_d (Table 3 and Table 5); B_d = 0.662, 0.658 and 0.543 for solutions 1, 2 and 3, respectively.

In the third (time-history) approach, seven historical accelerograms that were considered in the Cali microzonation [Decreto 158 2014] have been selected. Such inputs were recorded in rock; thus, they have been scaled [Kottke, Rathje 2008] to correspond to soil D and to match the aforementioned design spectrum for Cali. This scaling follows the guidelines of the Colombian regulation [NSR-10 2010].

Table 9 displays the maximum displacements in the isolation layer corresponding to the three analyzed isolation solutions (Table 8) and the three aforementioned analysis approaches.

Table 9. Maximum displacement (D_D) in the isolation layer (cm)			
Solution No.	**Equivalent forces according to ASCE 7-10**	**Equivalent forces method using the derived B_d factor**	**Time-history analysis**
1	26.41	24.20	22.32
2	24.81	24.27	21.93
3	21.93	20.22	15.52

Table 9 shows that the proposed formulation (third column) provides better agreement with the allegedly more exact dynamic results (last column) than the formulation contained in the American regulations [ASCE 7-10 2010] (second column). This can be read as a verification of a better suitability of the proposed formulation to the particular Colombian conditions.

8 CONCLUSIONS

This study proposes a strategy to derive damping modification factors after linear dynamic analyses by using artificial inputs that are generated to match the 5%-damped code design response spectra of the area under consideration. Given the sensitivity of such modification factors to the significant (Trifunac) duration, the considered artificial inputs are generated caring that this duration does not exceed significantly the one of the available local records. This approach is intended for any country, region or city where a sufficient number of representative seismic records is not readily accessible. The derived expressions are aimed to modify 5%-damped displacement (or pseudo-acceleration) and acceleration response spectra according to the actual value of the damping ratio of the analyzed construction; values both higher and smaller than 5% are considered.

The obtained expressions depend on the period; conversely, the influence of the soil type and the site seismicity is less relevant, being neglected in this study. The proposed modification factor for acceleration response spectra is greater than one for long periods and damping ratios higher than approximately 50%; this circumstance corroborates that, in buildings with base isolation, overdamping can lead to serious nonstructural damage.

An application example of the proposed strategy to Colombia is presented; expressions for scaling displacement and acceleration spectra are obtained. Such expressions match reasonably well those of the most relevant previous studies. The derived expressions are compared with other major seismic regulations, being concluded that lie within their range; noticeably, such codes show important scattering. The results obtained with these artificial inputs are compared with those for some available historical accelerograms recorded in Colombia; the agreement is rather satisfactory, accounting that such actual inputs are too scarce to represent the actual seismicity. Concerning seismic isolation, the current Colombian code refers to the USA regulations; although there are relevant discrepancies with the results of this study, the differences are only moderate for the ranges of period and damping of interest. The suitability of the proposed formulation to the Colombian situation is further analyzed in a verification example of a base-isolated hospital building; comparison with results derived after time-history analyses using actual inputs shows better agreement than using the US regulations.

The satisfactory performance of the derived expressions shows that artificial accelerograms can be a convenient option to estimate the damping modification factor in countries without enough actual seismic records, like Colombia.

ACKNOWLEDGEMENTS

This work has received financial support from Spanish Government under projects BIA2014-60093-R and CGL2015-6591. The stay of the PhD candidate C. Piscal at Barcelona has been funded by Colciencias (Colombian government) under call 617. These supports are gratefully acknowledged.

REFERENCES

- Anbazhagan P, Uday A, Moustafa SS, Al-Arifi NS. (2016). Pseudo-Spectral Damping Reduction Factors for the Himalayan Region Considering Recorded Ground-Motion Data. *PloSone*, **11**(9):e0161137.
- Arias A. (1970). A measure of earthquake intensity. Seismic Design for Nuclear Power Plants. MIT Press, 438–483.
- ASCE 7-10 (2010). *Minimum design loads for buildings and other structures*. American Society of Civil Engineers.
- ASCE 7-16 (2016). *Minimum design loads and associated criteria for buildings and other structures*. American Society of Civil Engineers.
- ATC-40. (1996). *Seismic evaluation and retrofit of concrete buildings*. Applied Technology Council, Redwood City, CA.
- Atkinson GM, Pierre JR. (2004). Ground-motion response spectra in eastern North America for different critical damping values. *Seismological Research Letters*, **75**(4):541-545.
- Benahmed B, Hammoutene M, Cardone D. (2016). Effects of Damping Uncertainties on Damping Reduction Factors. *Periodica Polytechnica Civil Engineering*.
- Benavent-Climent A, Pujades LlG, López Almansa F. (2002). Design energy input spectra for moderate seismicity regions. *Earthquake Engineering and Structural Dynamics*, **31**:1151-1172.
- Benavent Climent A, López Almansa F, Bravo González DA. (2010). Design energy input spectra for moderate-to-high seismicity regions based on Colombian earthquakes. *Soil Dynamics & Earthquake Engineering*, **30**(11):1129-1148.
- Bommer JJ, Mendis R. (2005). Scaling of displacement spectral ordinates with damping ratios. *Earthquake Engineering and Structural Dynamics*, **34**(2):145–165.
- Bradley BA. (2015). Period dependence of response spectrum damping modification factors due to source- and site-specific effects. *Earthquake Spectra*, **31**(2):745-759.
- BSL (2009). *The Building Standard Law of Japan*. Ministry of Land, Infrastructure, Transport and Tourism.
- Cameron WI, Green RA. (2007). Damping correction factors for horizontal ground-motion response spectra. *Bulletin of the Seismological Society of America*. **97**(3):934-960.
- Cardone D, Dolce M, Rivelli M. (2009). Evaluation of reduction factors for high-damping design response spectra. *Bulletin of Earthquake Engineering*, **7**:273–291.
- Cassarotti C, Monteiro R, Pinho R. (2009). Verification of spectral reduction factors for seismic assessment of bridges. *Bulletin of the New Zealand Society for Earthquake Engineering*, **42**(2):111.
- Decreto 158. (2014). *Microzonificación sísmica de Santiago de Cali*. Santiago de Cali, (in Spanish).
- EN-1998 (2004). *Eurocode 8 - Design of structures for earthquake resistance*. European committee for standardization.
- FEMA P 1050. (2016). *NEHRP Recommended Seismic Provisions for New Buildings and Other Structures*. Federal Emergency Management Agency.
- GB 50011 (2010). *National Standard of the People's Republic of China*. China Architecture & Building Press.
- Gulkan P, Sozen M. (1974). Inelastic response of reinforced concrete structures to earthquake ground motions. *ACI Journal*, 71:604–610.
- Hao AM, Zhou DY, Li YM. (2011). Effects of moment magnitude, site conditions and closest distance on damping modification factors. *Soil Dynamics and Earthquake Engineering*, **31**:1232–1247.
- Hatzigeorgiou GD. (2010). Damping modification factors for SDOF systems subjected to near-fault, far-fault and artificial earthquakes. *Earthquake Engineering and Structural Dynamics*, **39**(11):1239-1258.
- Housner G.W. (1952). Spectrum intensities of strong-motion earthquakes. *Symposium on earthquakes and blast effects on structures, Los Angeles*.
- Kelly JM. (1999). The role of damping in seismic isolation. *Earthquake Engineering and Structural Dynamics*, **28**:3-20.
- Kottke A, Rathje E. (2008). A Semi-Automated Procedure for Selecting and Scaling Recorded Earthquake Motions for Dynamic Analysis. *Earthquake Spectra*, 24(4):911–932.
- Lin YY, Chang KC. (2003). Study on Damping Reduction Factor for Buildings under Earthquake Ground Motions. *Journal of Structural Engineering ASCE*, **130**(11):206-214.
- Lin YY, Chang KC. (2004). Effects of Site Classes on Damping Reduction Factors. *Journal of Structural Engineering ASCE*, **129**(2):1667-1675.
- Lin YY, Miranda E, Chang KC. (2005). Evaluation of damping reduction factors for estimating elastic response of structures with high damping. *Earthquake Engineering and Structural Dynamics*, **34**(11):1427-1443.
- Lin YY. (2007). Statistical study on damping modification factors adopted in Taiwan's seismic isolation design code by using the 21 September 1999 Chi-Chi earthquake, Taiwan. *Engineering Structures*, **29**:682–693.

- López Almansa F, Yazgan U, Benavent Climent A. (2013). Design energy input spectra for high seismicity regions based on Turkish registers. *Bulletin of Earthquake Engineering*, **11**(4):885–912.
- Mavroeidis GP. (2015). Discussion on "Displacement damping modification factors for pulse-like and ordinary records". *Engineering Structures*, **100**: 249–252.
- Mendo A, Fernandez-Dávila VI. (2017). Bases for standard of analysis and design of base isolation system for buildings in Peru. *16th World Conference on Earthquake Engineering, Santiago de Chile*.
- Mollaioli F, Liberatore L, Lucchini A. (2014). Displacement damping modification factors for pulse-like and ordinary records. *Engineering Structures*, **78**:17-27.
- NCh 2745. (2013). *Análisis y diseño de edificios con aislación sísmica*. Asociación Chilena de Sismología e Ingeniería Sísmica. Instituto Nacional de Normalización.
- NSR-10. (2010). Reglamento Colombiano de Construcción Sismo Resistente. Asociación Colombiana de Ingeniería Sísmica.
- Palermo M, Silvestri S, Trombetti T. (2016). Stochastic-based damping reduction factors. *Soil Dynamics and Earthquake Engineering*, 80:168–176.
- Piscal A. C, López Almansa F. (2016). Consequences of the possible application to Colombia of the most recent codes on seismic isolation of buildings. *Revista Internacional de Ingeniería Estructural* **21**:415–436.
- Piscal A. C. (2018). Basis for the proposal of Colombian design code for buildings protected with base isolation or energy dissipators. Doctoral Dissertation. Technical University of Catalonia.
- Priestley MJN. (2003). *Myths and fallacies in earthquake engineering, revisited*. IUSS Press, Pavia (Italy).
- Priestly MJN, Calvi GM, Kowalski MJ. (2007). *Displacement-based seismic design of structures*, IUSS Press.
- Pu W, Kasai K, Kabando EK, Huang B. (2016). Evaluation of the damping modification factor for structures subjected to near-fault ground motions. *Bulletin of Earthquake Engineering*, **14**(6):1519-1544.
- Ramírez OM, Constantinou MC, Kircher CA, Whittaker AS, Johnson MW, Gomez JD, Chrysostomou CZ. (2001). Development and evaluation of simplified procedures for analysis and design of buildings with passive energy dissipation systems, *Report MCEER 00-0010, State University of New York at Buffalo*.
- Ramírez OM, Constantinou MC, Whittaker AS, Kircher CA, Chrysostomou CZ. (2002). Elastic and Inelastic Seismic Response of Buildings with Damping Systems. *Earthquake Spectra*, **18**(3)531–547.
- RSNC (2017). Red Sismológica Nacional de Colombia (Colombian Seismological National Network), http://seisan.sgc.gov.co/RSNC/.
- Rezeian S, Bozorgnia Y, Idriss IM, Abrahamson N, Campbell K, Silva W. (2014). Damping scaling factors for elastic response spectra for shallow crustal earthquakes in active tectonic regions: "Average" horizontal component. *Earthquake Spectra*, **30**(2):939–63.
- Saragoni R, Hart GC. (1973). Simulation of artificial earthquakes. *Earthquake Engineering and Structural Dynamics* **2**:249–267.
- Sáez A, Moroni MO, Sarrazin M. (2012). Contributions to the Chilean Code for Seismic Design of Buildings with Energy Dissipation Devices. *15th World Conference on Earthquake Engineering, Lisbon*.
- Seismosoft (2016). *SeismoArtif - A computer program for generation of artificial accelerograms*. Available from URL: www.seismosoft.com.
- Sheikh MN, Tsang HH, Yaghmaei-Sabegh S, Anbazhagan P. (2013). Evaluation of damping modification factors for seismic response spectra. *Australian Earthquake Engineering Society Conference, Tasmania*.
- Shibata A, Sozen M (1976). Substitute-structure method for seismic design in RC. *Journal of Structural Engineering ASCE*, **102**:1–18.
- Stafford PJ, Mendis R, Bommer JJ. (2008). The dependence of spectral damping ratios on duration and number of cycles. *Journal of the Structural Engineering (ASCE)*, **134**(8):1364–1373.
- Trifunac MD, Brady AG. (1975). A study on the duration of strong earthquake ground motion. Bulletin of the Seismological Society of America **65**(3):581-626.
- Williams T, Kelley C. (2011). Gnuplot 4.5: an interactive plotting program. URL http://gnuplot.info. (Last accessed: May 2017).